

Resonance Scattering Technique and break-up to study nuclear structure

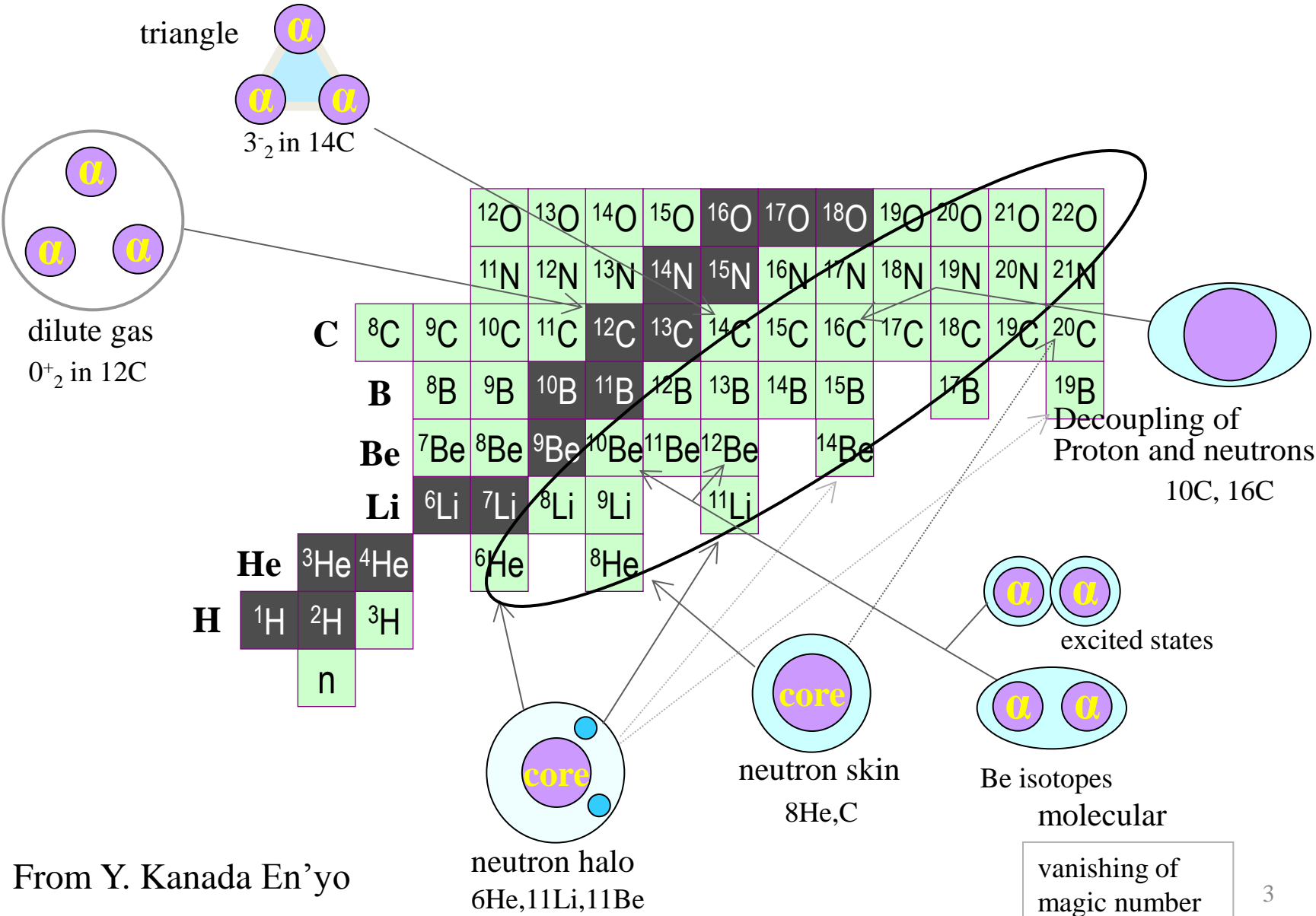
A. Di Pietro



Outline of the lecture:

- **Resonance scattering method in reverse kinematics.**
- **Advantages of the technique.**
- **Resolution. Discrimination of different processes and energy reconstruction.**
- **Resonant break-up**
- **3-body kinematics**

Exotic structures in light nuclei



From Y. Kanada En'yo

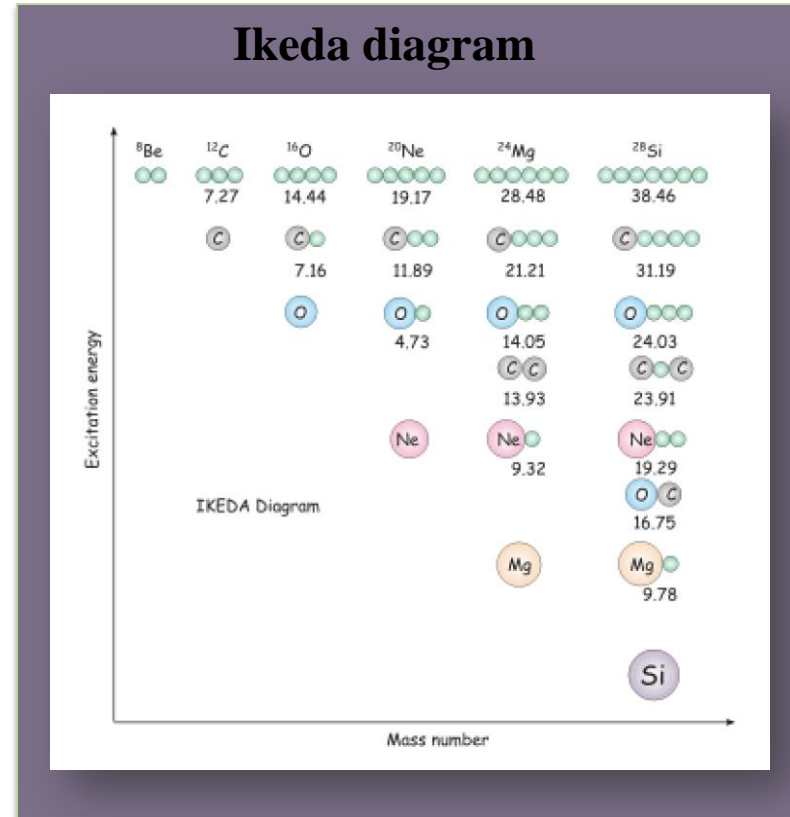
Conventional cluster structure

Cluster structure is a well established feature of many light $N \approx Z$ nuclei both in their ground and excited states.

Weak coupling picture:

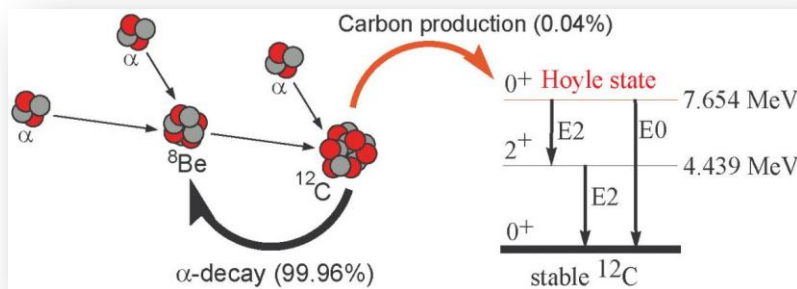
1. Clusters are formed by tightly bound nucleons (cluster is stiff, i.e. not easy to excite);
2. Weakly coupled inter-cluster motion is considered.

Threshold rule: i.e. these states appear close to the threshold for breaking-up into the cluster constituents.



K. Ikeda et al. Supp.Progr.Theo.Phys. 68(1980)1

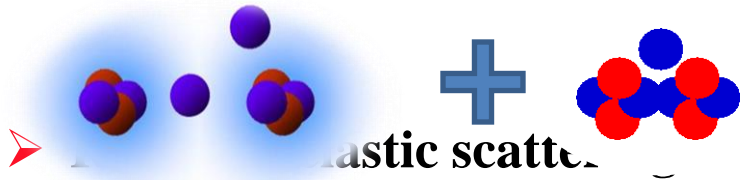
Ex. Hoyle state in ^{12}C



Possible ways to study cluster structures:

➤ transfer and decay into the constituents

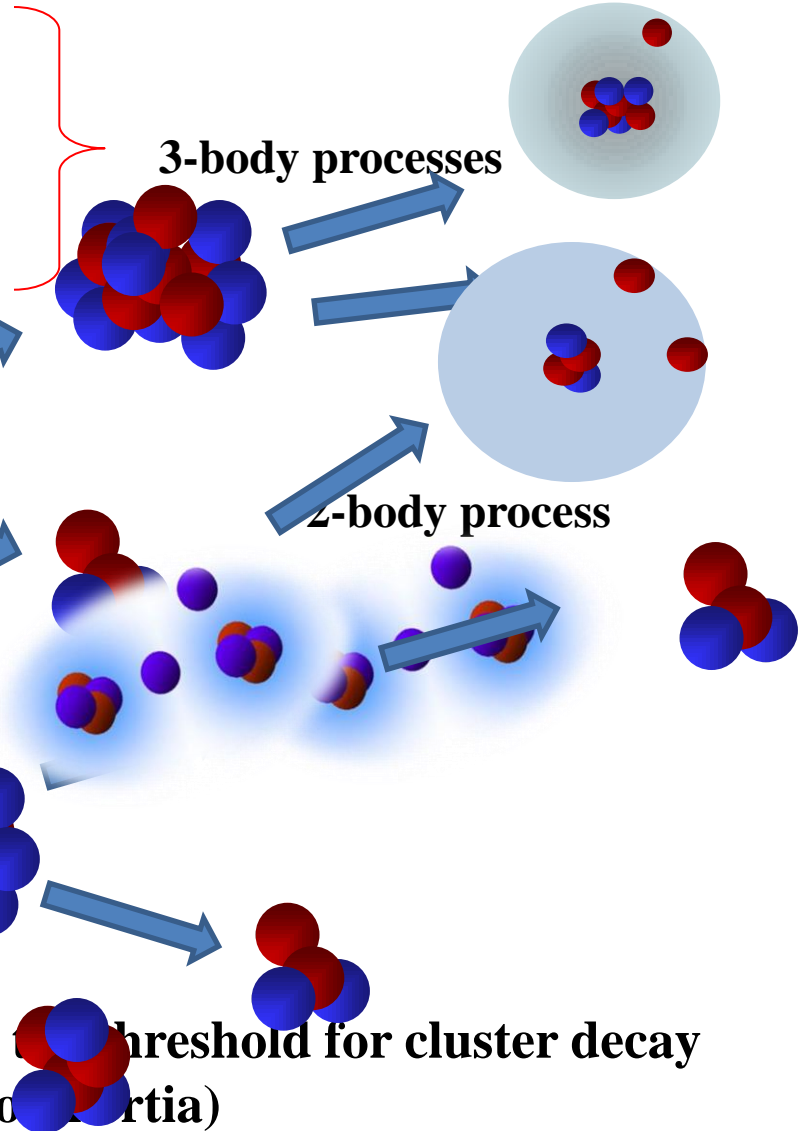
➤ inelastic scattering followed by break up



Ex: $^{10}\text{Be} + b \rightarrow ^6\text{He} + \alpha + b$
 Ex: $^{10}\text{Be} + \alpha \rightarrow ^{14}\text{C}^* \rightarrow ^{10}\text{Be} + \alpha$



➤ rotational bands with band head around threshold for cluster decay (measurement of E_{exc} and $J^\pi \rightarrow$ moment of inertia)



Resonant scattering method (RSM) in inverse kinematics

K.P.Artemov et al. Sov.J.Nucl.Phys. 52(1990)408

Elastic scattering of heavy projectiles **B** on a light targets **b** (protons or α s) in order to study properties of the compound nucleus **C** resulting from



Excitation function measured at $\theta_{\text{cm}} \approx 180^\circ \Rightarrow$ enhanced visibility of resonances with respect to potential and Coulomb scattering.

➤ thick solid or gaseous target

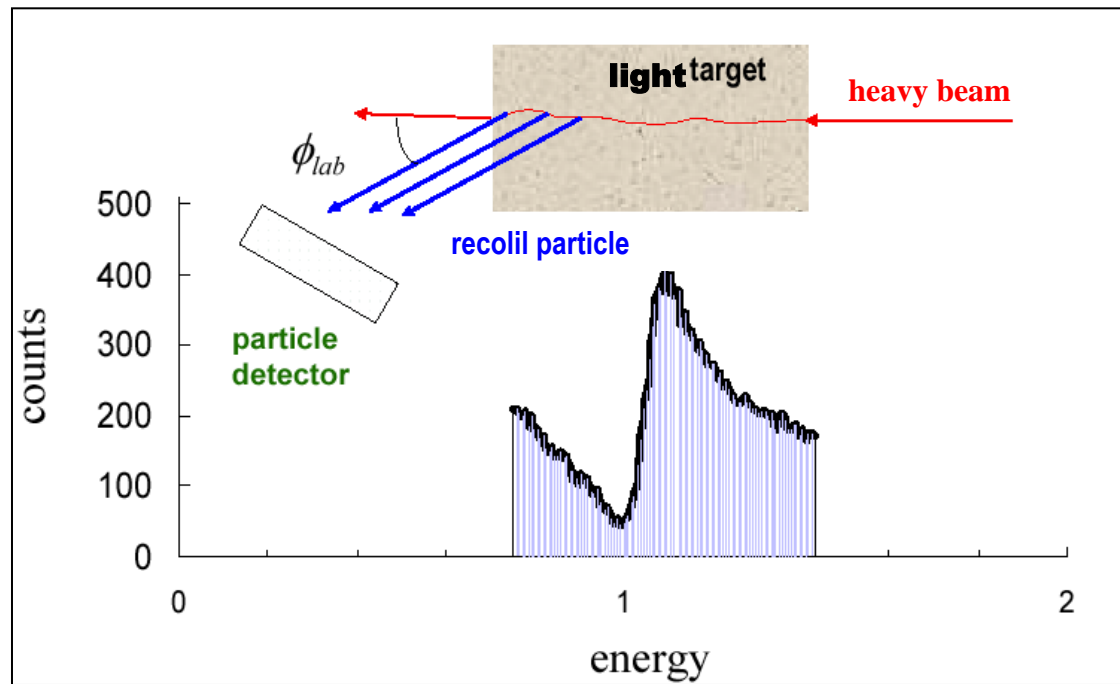
➤ gaseous target (H, He)



easy to change target thickness (changing gas pressure)

more homogeneous target

Used in the last ten years to measure excitation functions with radioactive beams.



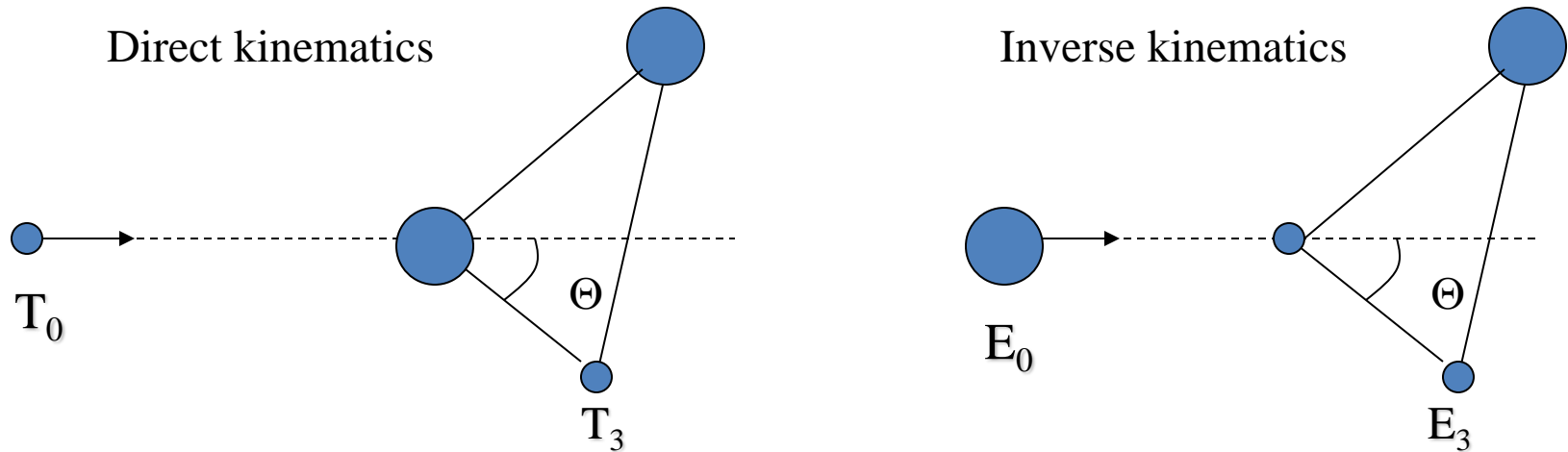
➤ Very useful in experiments with low intensity beams ($10^4 \div 10^6$ pps).

➡ Allows to measure excitation function in a wide energy range without changing beam energy ➔ reduces running time of the experiment

➡ Allows precise measurement of resonance properties: $E_r, J^\pi, \Gamma_{tot}, \Gamma_p, \Gamma_{\alpha}$

➡ Allows to measure recoil particles around $\theta_{c.m.} \sim 180^\circ$

Advantages of using inverse kinematics



E_0 e T_0 = laboratory projectile energy in direct and reverse kinematics respectively

E_0' e T_0' = c.m. energy in direct and reverse kinematics respectively

Θ =laboratory scattering angle of light particle

E_3 e T_3 = light particle laboratory energy in direct and reverse kinematics respectively

Some trivial equations (see previous lecture)

$$T_0' = T_0 \frac{M}{m+M} \quad \text{direct}$$

$$E_0' = E_0 \frac{m}{m+M} \quad \text{inverse}$$

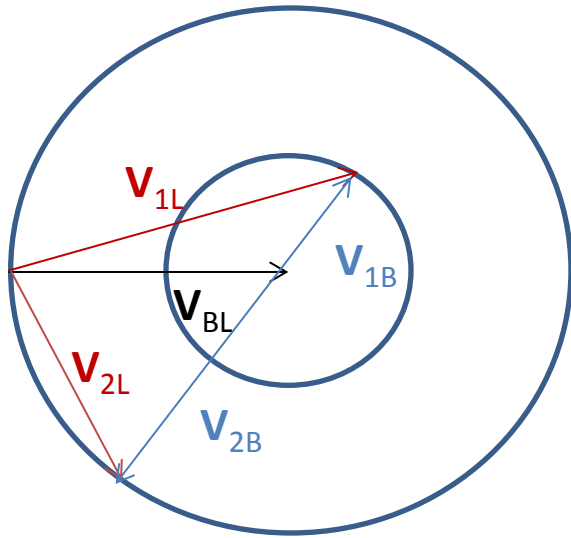
For the same c.m. energy:

$$\mathbf{T}_0' = \mathbf{E}_0' \rightarrow \left(\frac{E_0}{T_0} = \frac{M}{m} \equiv k \right)$$

For: $\theta_{\text{lab}} = 0^\circ$ ($= 180^\circ$ in the c.m.) \Rightarrow light particle energy is:

$$T_3 = T_0 \left(\frac{m}{m+M} \right)^2 (k+1)^2$$

$$E_3 = 4E_0 \frac{mM}{(m+M)^2}$$



In the current notation :

$E_3 = E_{2L}$ recoil energy in the Lab system

$E_{1L} = E_0$ projectile energy

$$E_3 = E_{2L} = \frac{1}{2} m V_{2L}^2 = \frac{1}{2} m (V_{BL}^2 + V_{2B}^2 - 2V_{BL} V_{2L} \cos \theta_{1B}) =$$

$$= \frac{1}{2} m 4V_{BL}^2 = 4 \frac{1}{2} m V_{BL}^2 \quad \text{at } \theta_{1B} = 180^\circ$$

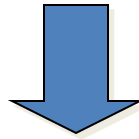
$$E_{cm} = \frac{m}{M+m} E_{1L}$$

$$E_{cm} = \frac{1}{2} \frac{mM}{m+M} V_{BL}^2 = \frac{m}{m+M} E_{1L} \Rightarrow \frac{1}{2} m V_{BL}^2 = \frac{mM}{(m+M)^2} E_{1L} \Rightarrow E_3 = 4 \frac{mM}{(m+M)^2} E_{1L}$$

Excitation function from measured recoil energy:



$$E_{ex} = E_{c.m.} + Q = E_0 \frac{m}{M+m} + Q$$



$$E_{ex} = \frac{M+m}{4M \cos^2(\theta_{lab})} E_3 + Q$$

Laboratory energy resolution for light recoil particles in inverse kinematics.

$$\varepsilon = \Delta E \frac{\left(\frac{dE}{dx}\right)_{li}}{\left(\frac{dE}{dx}\right)_{HI}} \approx \frac{\Delta E}{4} \frac{z^2}{Z^2}$$

ΔE =beam energy straggling in the laboratory

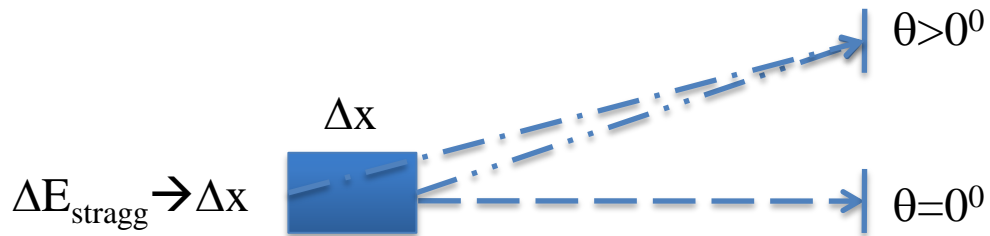
$(dE/dx)_{li}$ = stopping power for light particles

$(dE/dx)_{HI}$ = stopping power for beam particles

z = charge of light recoil particles

Z =charge of beam particles

Dependence of energy resolution from energy straggling

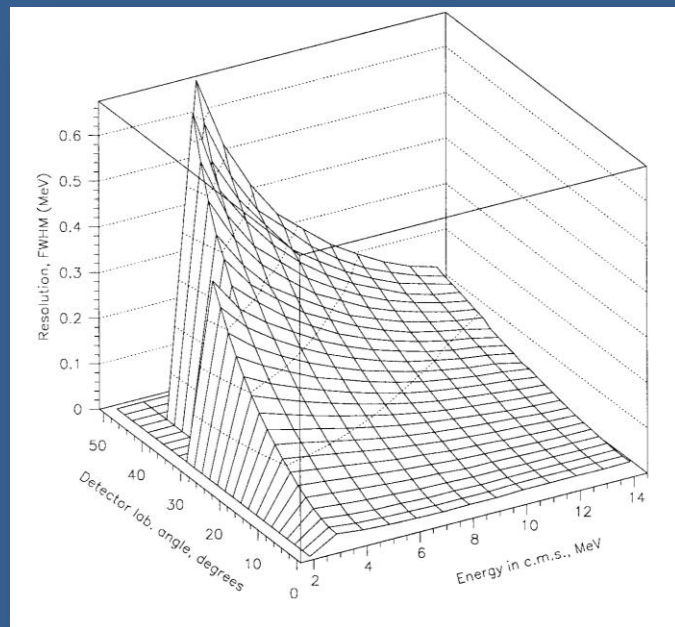


Due to energy straggling, to the same $E_{c.m.}$ correspond different $E_{det.}$ due to different paths.

Effect larger at $\theta > 0^\circ$ due to additional contribution of different scattering angles.

$^{32}\text{S} + \alpha$

G. Rogachev Ph.D thesis. Moscow1999

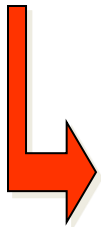


Energy resolution depends also from:

- Beam spot size
- Detector energy resolution
- Detector angular resolution
- Kinematical spread within $\delta\theta$
- Beam angular straggling
- Recoil angular straggling (small)

Problems of using this technique:

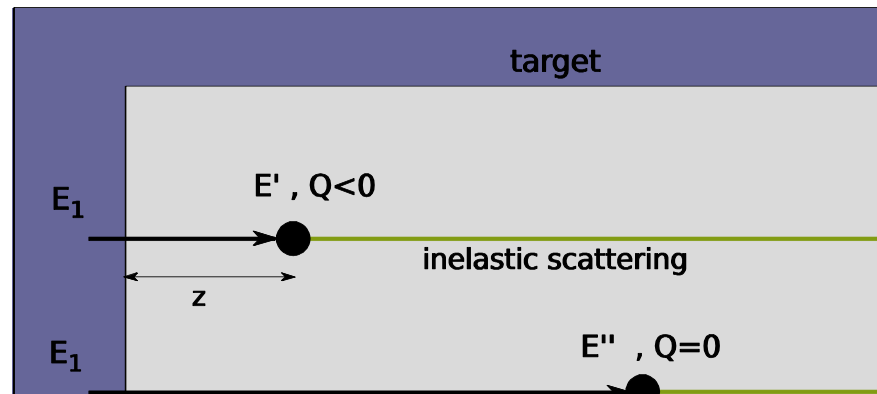
- Sources of background \Rightarrow inelastic scattering events
- Precise knowledge of stopping power to extract correctly the resonance parameters



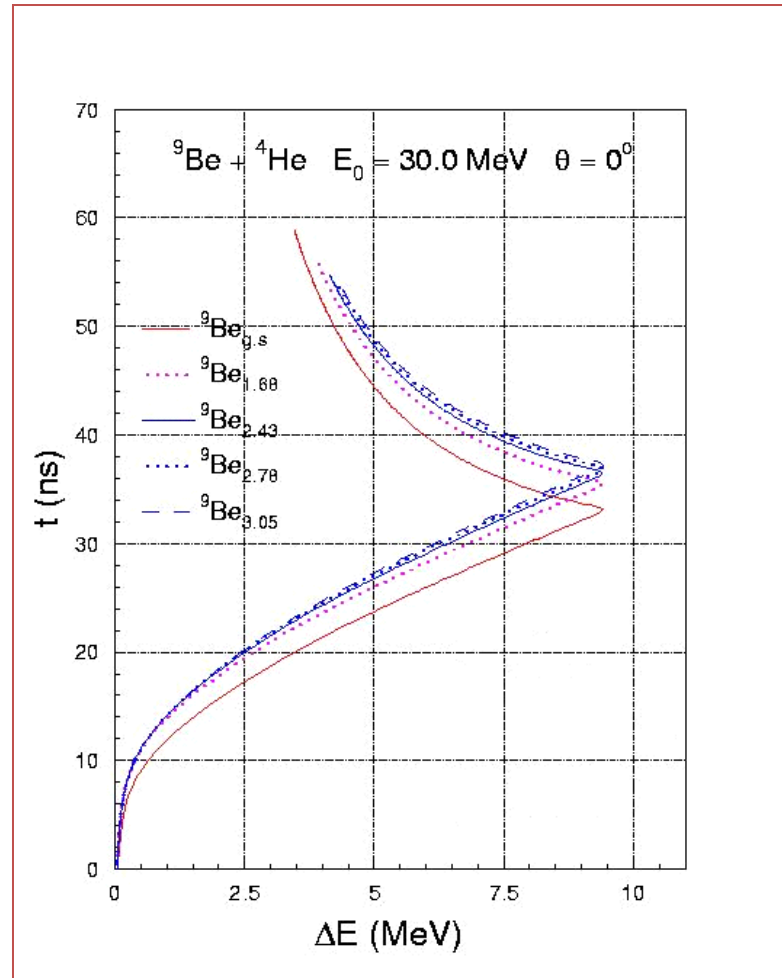
Need to measure de/dx with radioactive beams (but not only!)

How to discriminate elastic from inelastic scattering events?

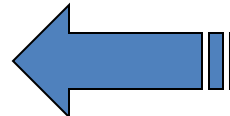
- ✓ From α or p spectrum no possibilities to discriminate the process which produces recoil particles.
- ✓ In experiment with a gaseous extended target is possible to discriminate elastic from inelastic from time of flight measurement or tracking (active targets).



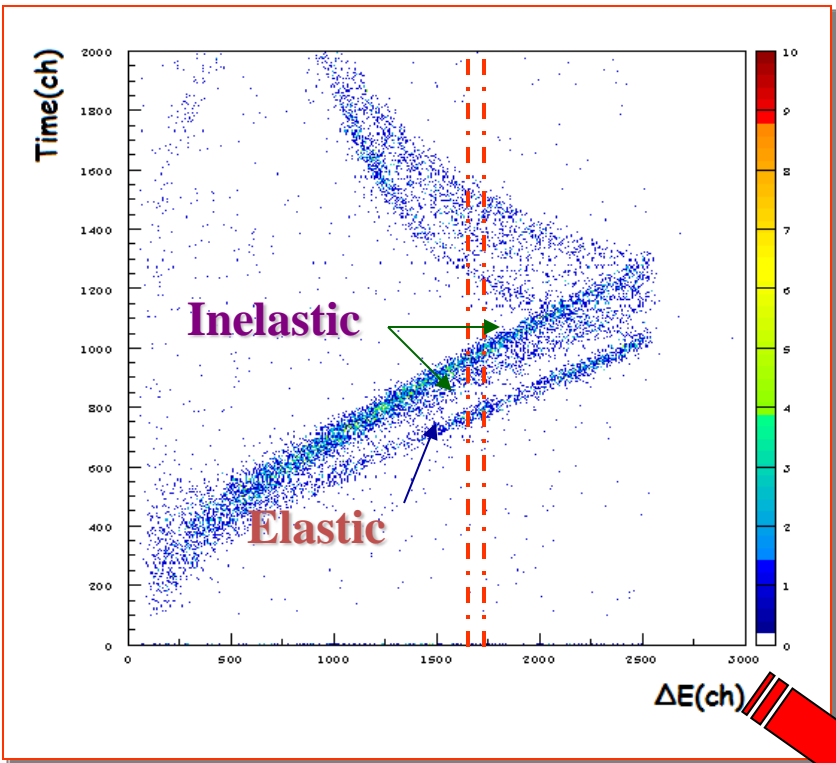
Example: ${}^9\text{Be} + {}^4\text{He}$



Calculated $T_{\text{tOF}} - \Delta E$ 2d-spectrum



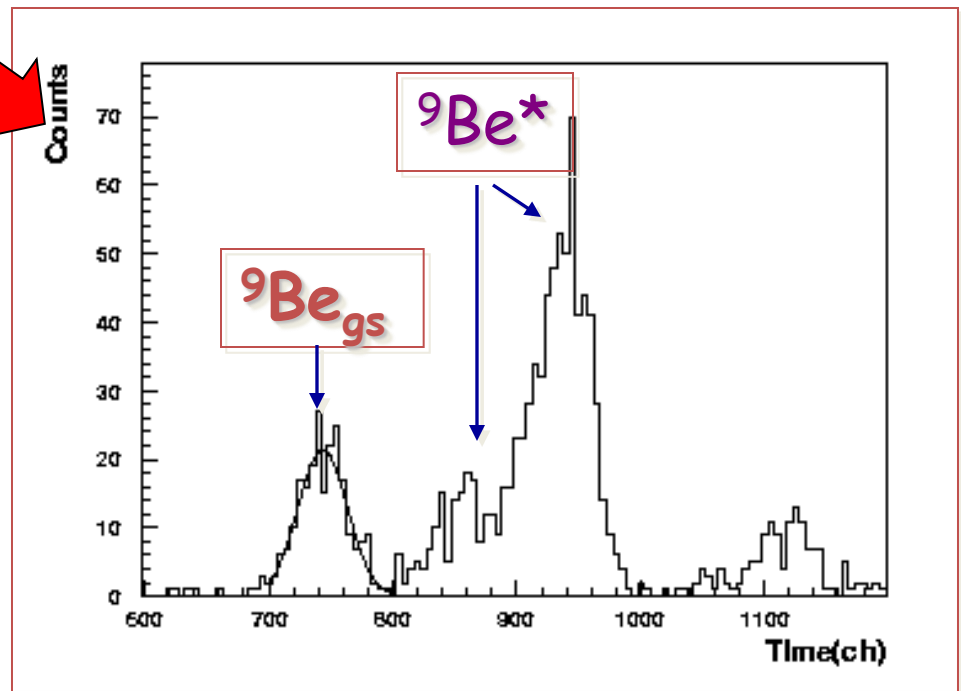
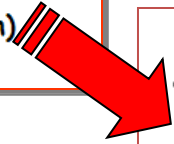
Experimental Ttof- ΔE
2d-spectrum



Projecting on time axis



Time resolution $\Delta T \sim 1$ ns

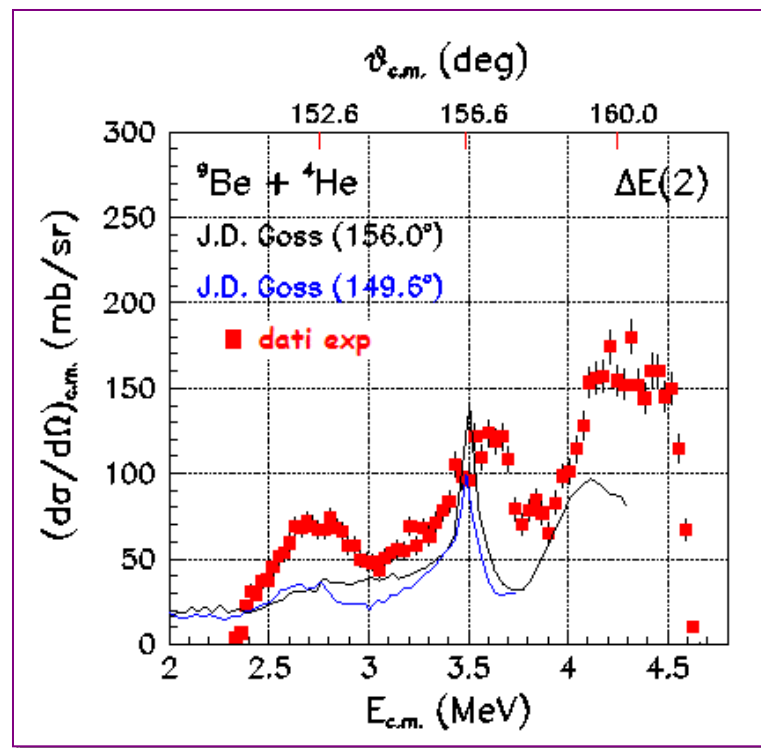
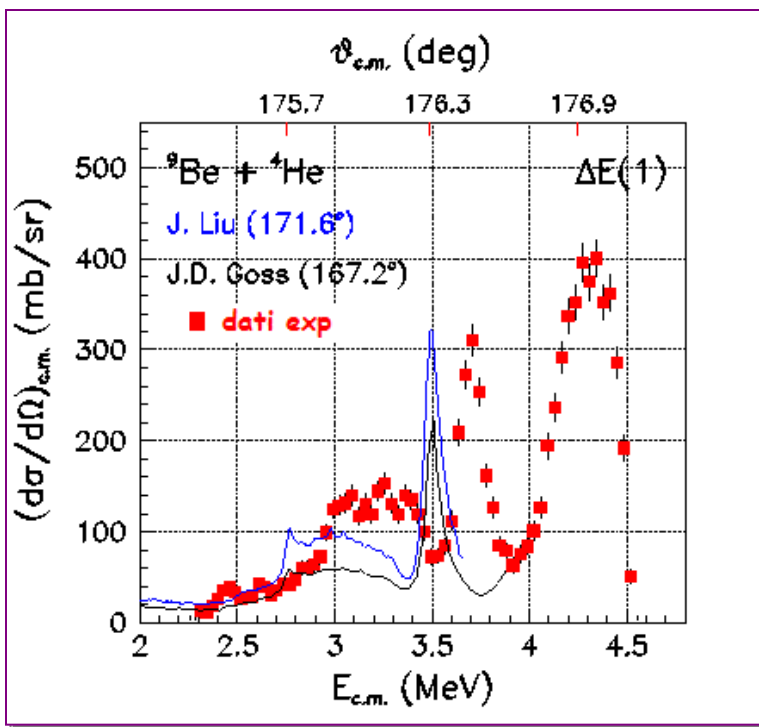


Problems with stopping power calculations.

Excitation function ${}^9\text{Be}+{}^4\text{He}$ at $E_{\text{cm}} < 4.5\text{MeV}$

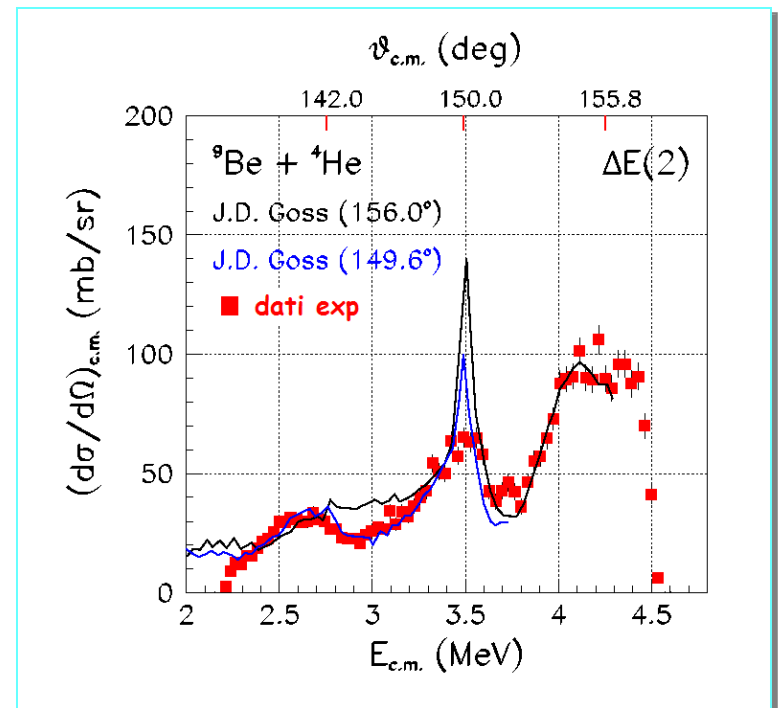
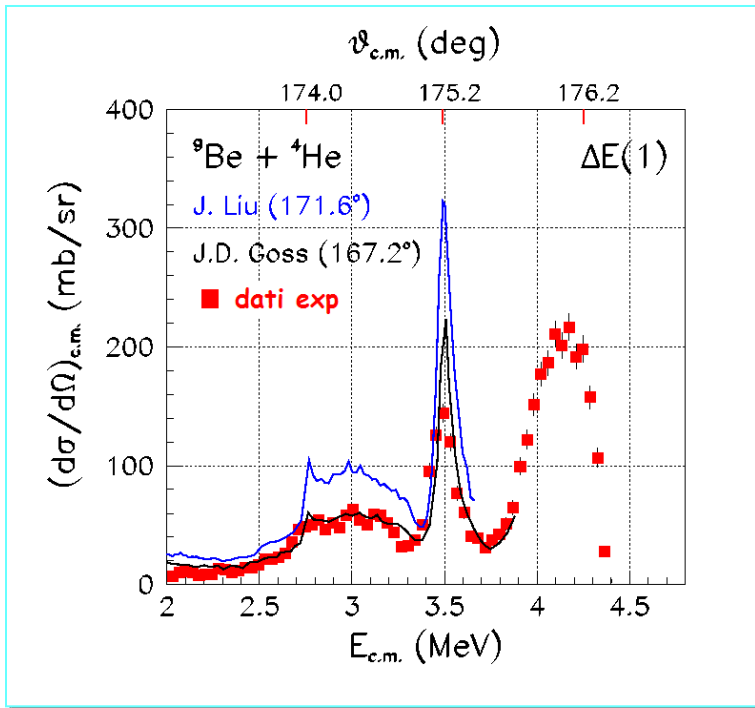
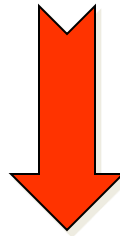
■ Excitation function ${}^9\text{Be} + \alpha$ with RSM on infinite target and energy loss calculated using Monte Carlo code SRIM M. Zadro et al, NIM B259 (2007).

— Excitation function $\alpha+{}^9\text{Be}$ measured with thin target method varying beam energy at small streps J. Liu [NIM B 108,(1996) 247] , J.D. Goss [PRC 7,(1973) 247]



Different energy resonance with the two techniques !

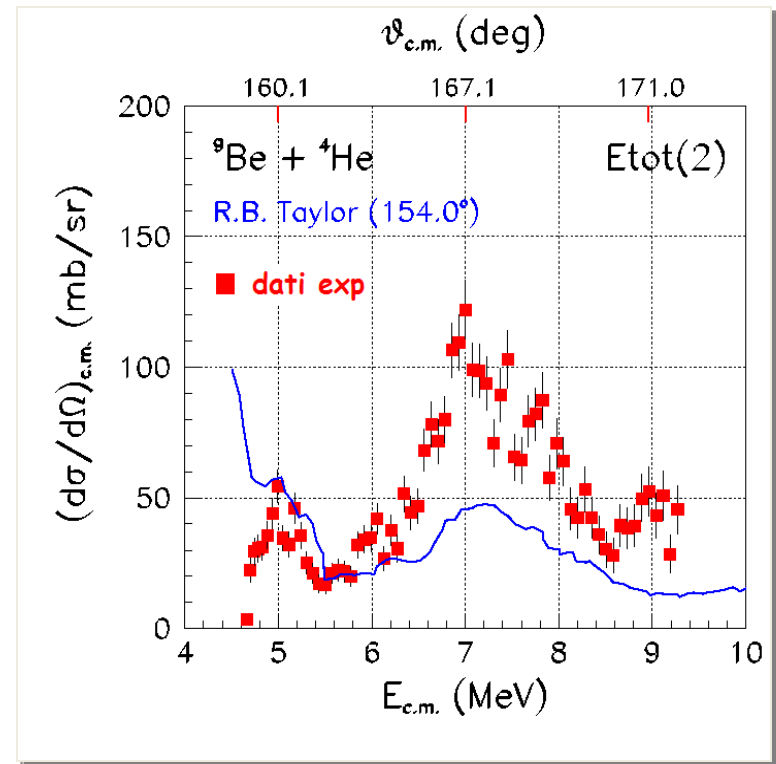
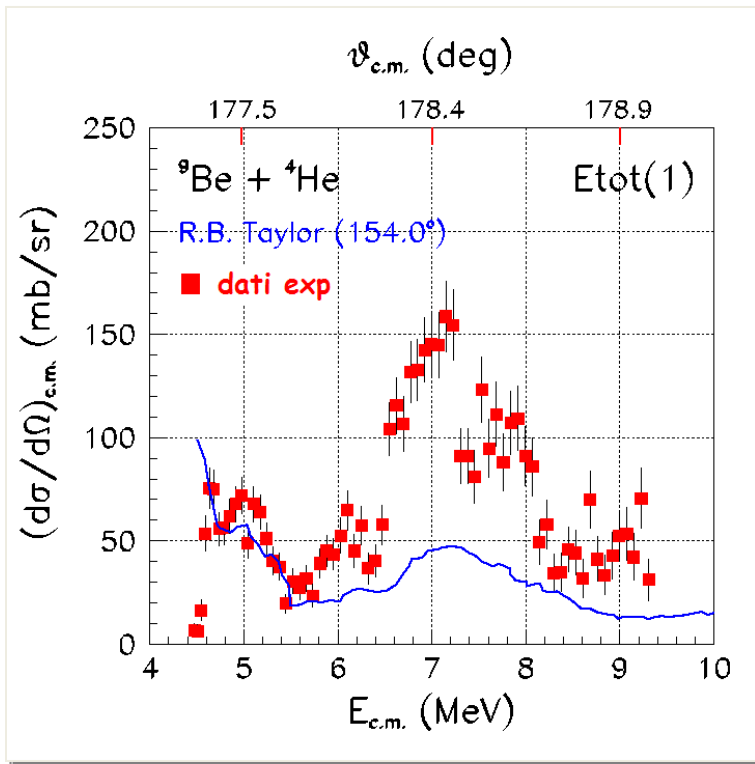
Using measured energy loss data



Note: changing stopping power data changes also extracted resonance cross-section

Excitation function ${}^9\text{Be} + \alpha$ at $E_{\text{cm}} > 4.5$ MeV

Using measured energy loss data



■ Excitation function ${}^9\text{Be} + \alpha$ with RSM on infinite target M. Zadro et al, NIM B259 (2007).

— Excitation function $\alpha + {}^9\text{Be}$ measured with thin target method varying beam energy at small streps R.B.Taylor [NP 65,(1965) 318]

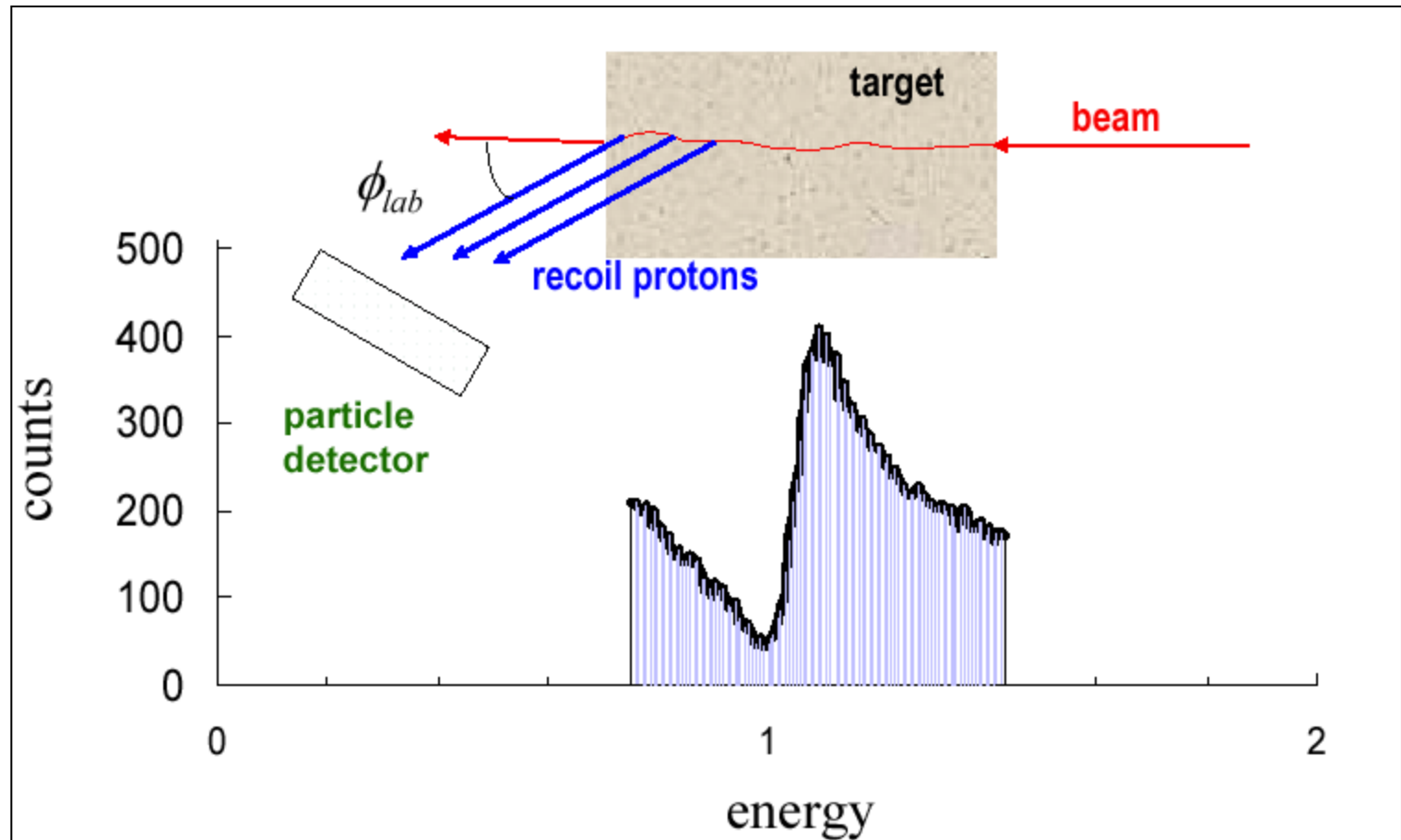
Need to measure stopping power with RIBs but not only!

**Some example of experiments performed using
RIBs and RSM technique.**

Level scheme of p-rich nuclei unknown for many species.

By bombarding a ^1H enriched target with a p-rich radioactive beam \Rightarrow possibility to study levels in the p-rich compound nucleus which are proton unbound.

RSM on thick target



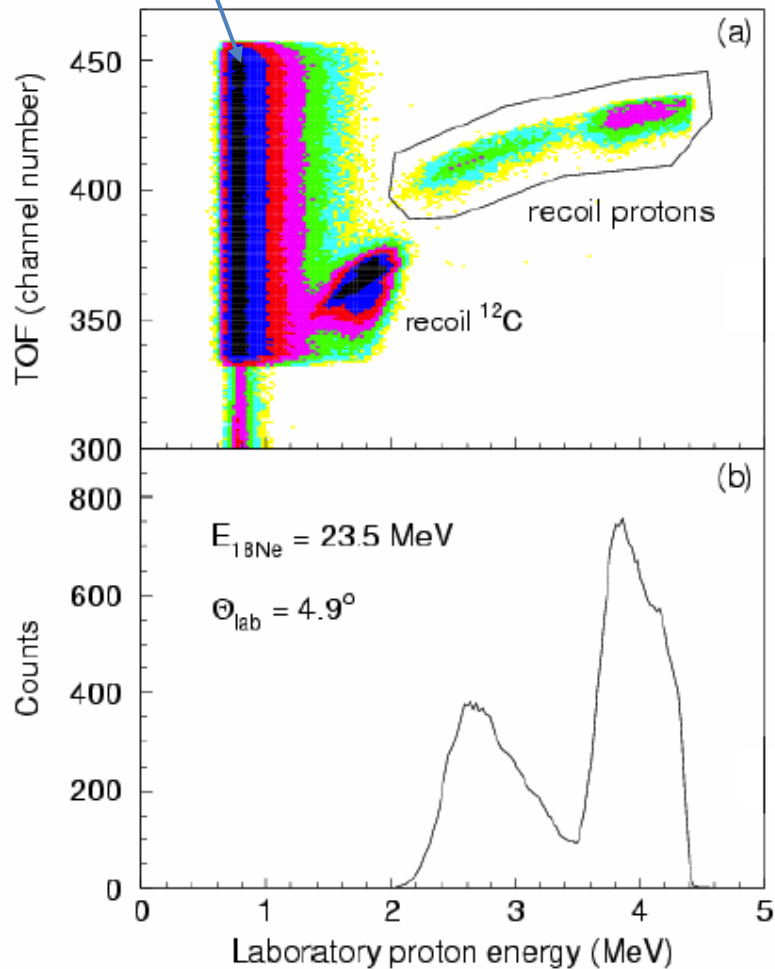
β background

Experiment performed at CRC Louvain-la Neuve

$^{18}\text{Ne} + \text{p}$ @ $E_{\text{lab}} = 21, 23.5$ and 28 MeV

Average beam intensity $\sim 4 \times 10^6$ pps

Target 0.5 mg/cm^2 polyethylene



Detection set-up

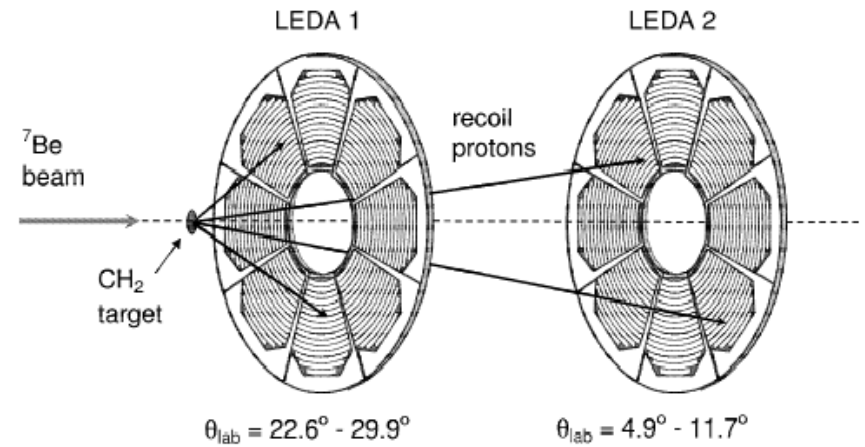


Fig. 1. Schematic drawing of the experimental set-up (see text).

C. Angulo et al. Nucl. Phys. A 716(2003)211

R-matrix analysis

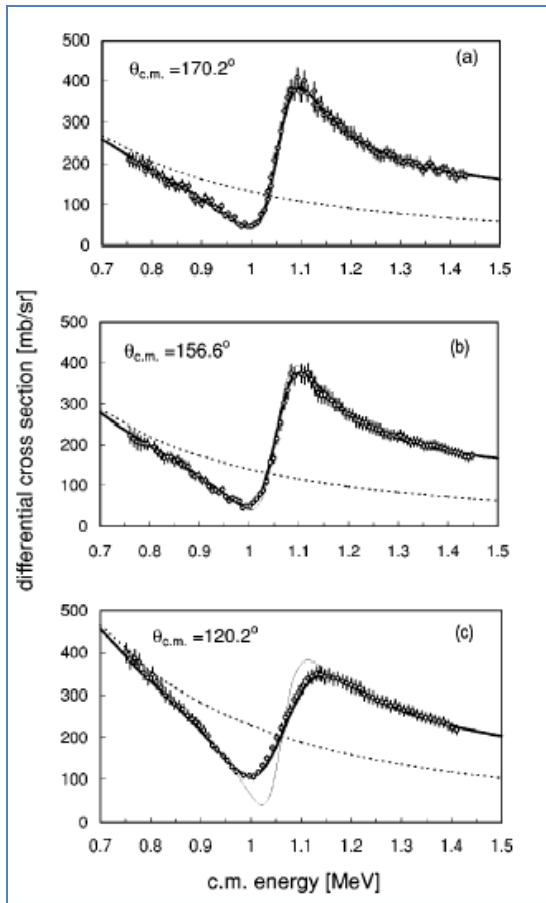
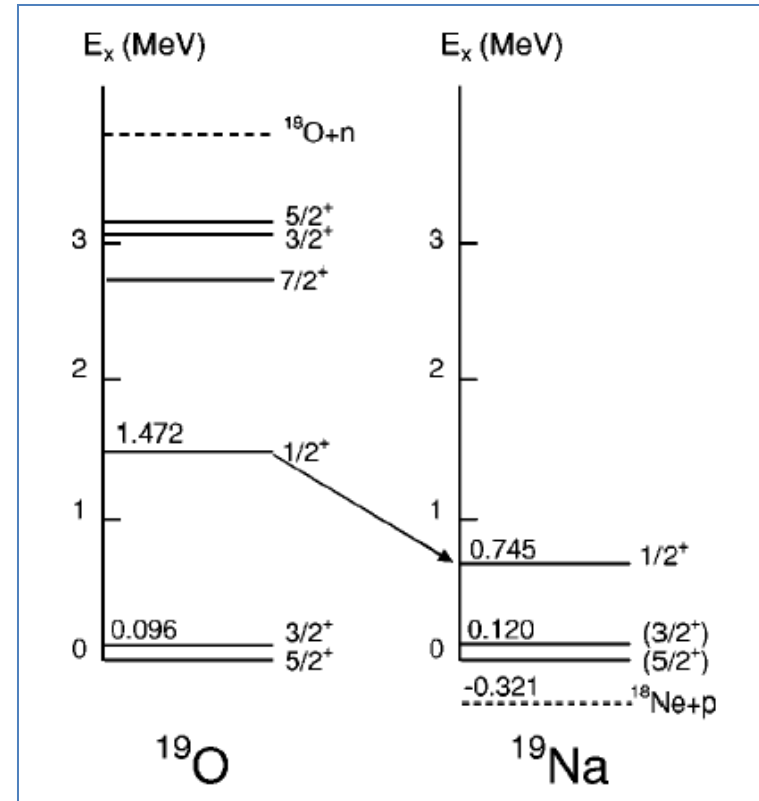


TABLE I. Results of the R -matrix fits ($N=367$).

	$a=4$ fm	$a=5$ fm	$a=6$ fm
E_R (MeV)	1.067 ± 0.003	1.066 ± 0.003	1.064 ± 0.003
Γ_p (keV)	104 ± 3	101 ± 3	95 ± 3
χ^2/N	0.53	0.44	0.49
θ_p^2 (%)	29.8	22.9	21.6

Level scheme

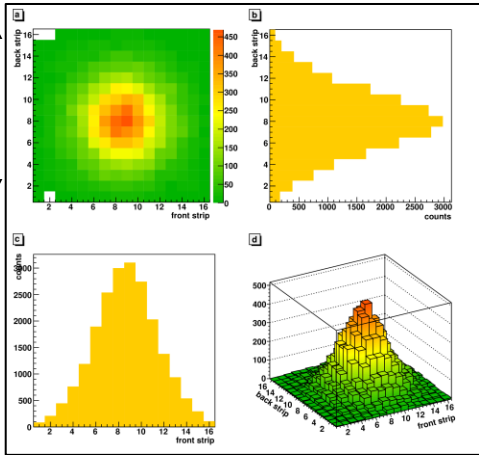


Very large Coulomb shift (~ 0.73 MeV) typical of deformed states in nuclei near the drip-line.

Beam profile

50 mm

50 mm

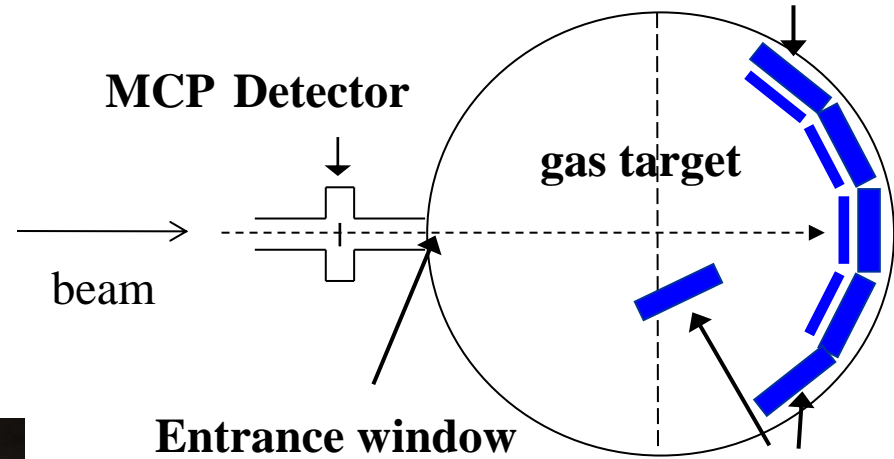


P=700 mbar

T=295 K

$E_{8\text{Li}}=30.6 \text{ MeV}$ $I \approx 5 \times 10^4 \text{ pps}$

$\Delta E + \text{DSSSD}$
detectors



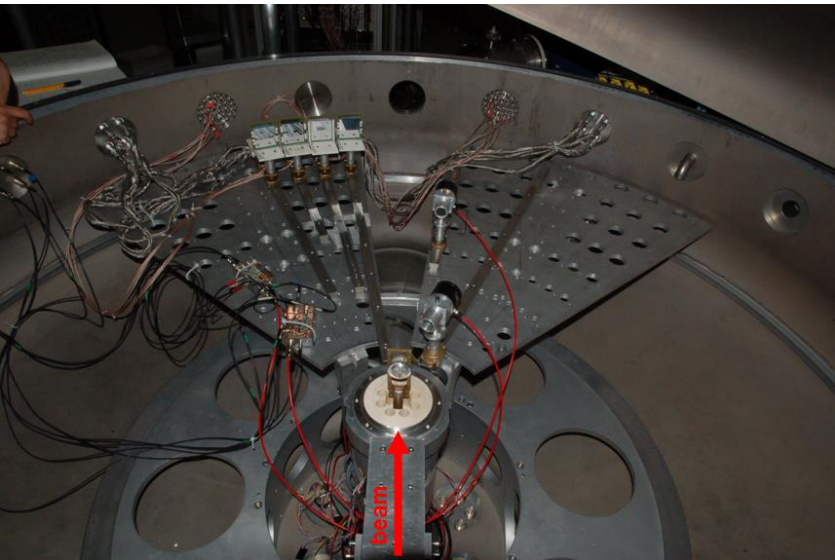
MCP Detector

beam

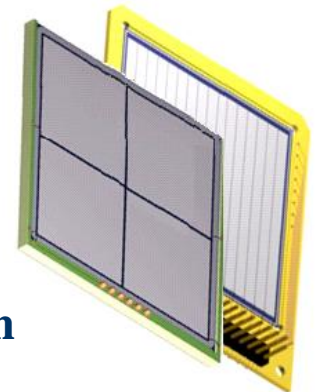
Entrance window

gas target

Stopping power
detectors



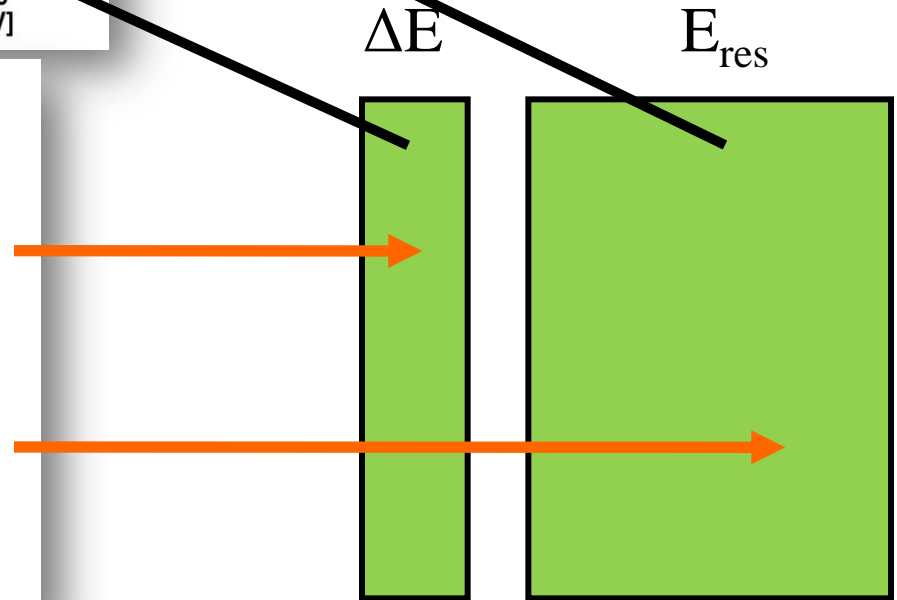
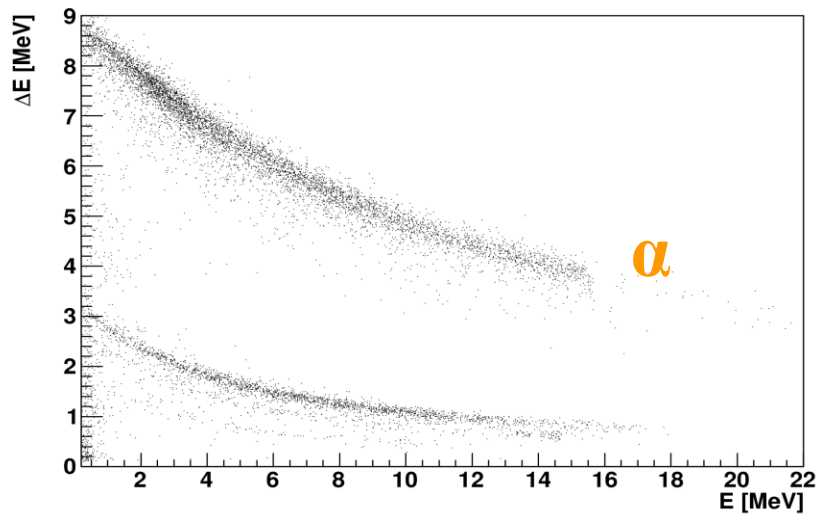
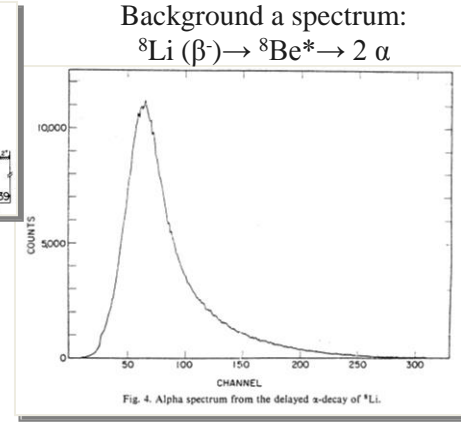
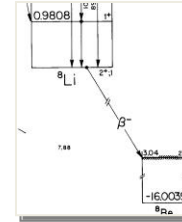
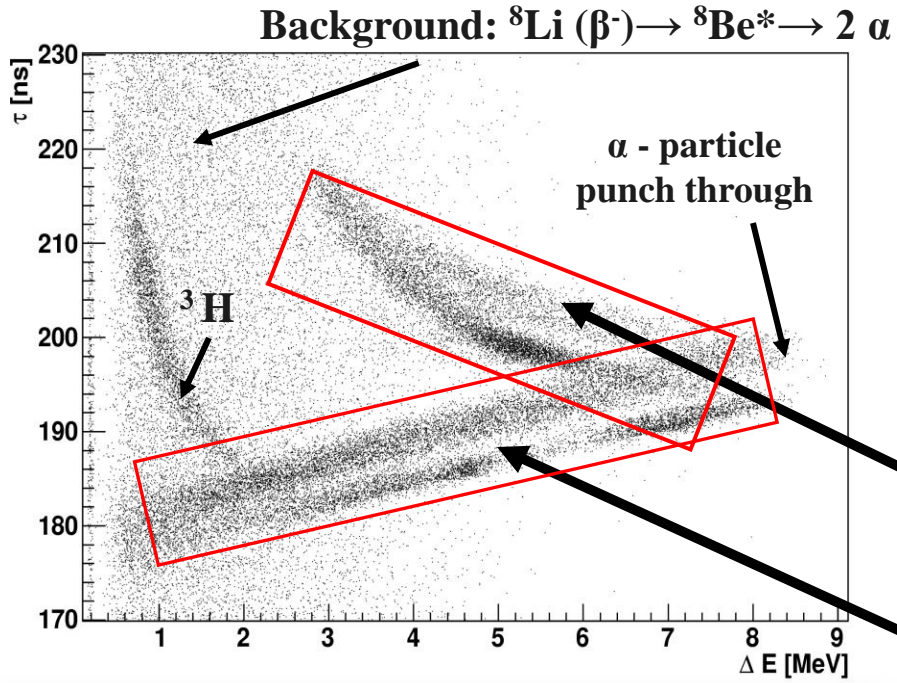
α



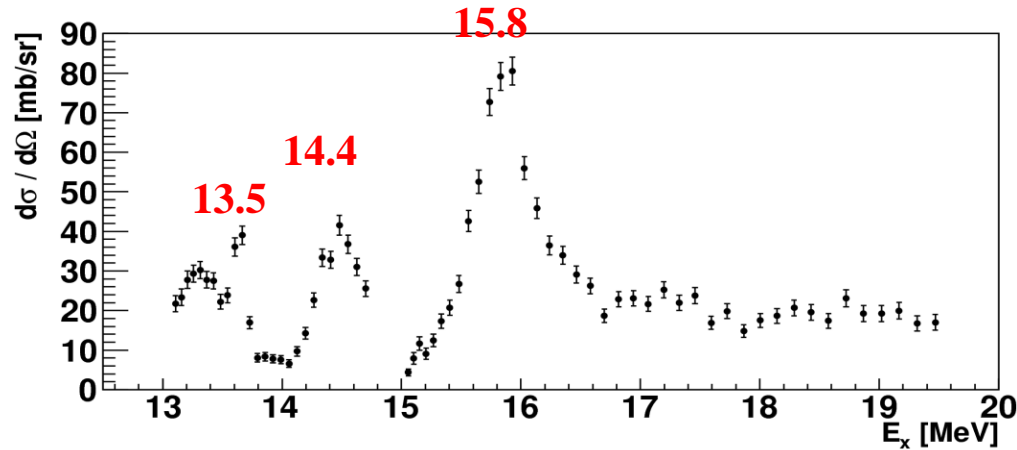
✓ ΔE : quadrants $50 \times 50 \text{ mm}^2$ quadrants Si detectors $50 \mu\text{m}$ thick.

✓ E Double Sided Silicon Strip Detectors, $50 \times 50 \text{ mm}^2$ 16+16 strip, $1000 \mu\text{m}$

Elastic scattering α particle discrimination

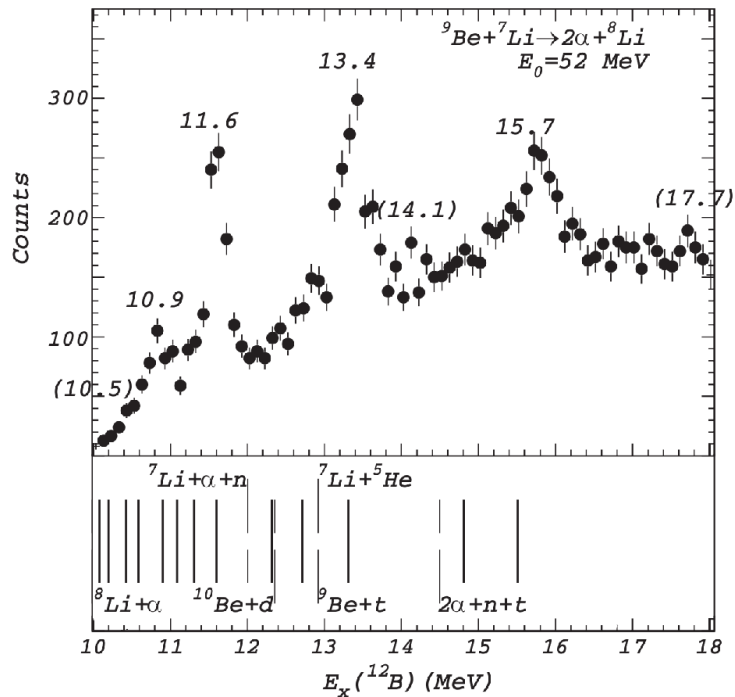


Comparison with literature



${}^{12}\text{B}$ states.

α particle threshold 10.0 MeV



E MeV	Err keV	Width keV	$J^\pi; T$	reazione
13.33	30	50 ± 20		${}^9\text{Be}({}^7\text{Li}, \alpha)$
13.40	100	Broad		${}^{10}\text{B}(t, p)$
13.4				${}^9\text{Be}({}^7\text{Li}, 2\alpha)$
14.1				${}^9\text{Be}({}^7\text{Li}, 2\alpha)$
14.80	100	< 200	$2+; 2$	${}^{14}\text{C}(p, {}^3\text{He})$
15.50				${}^9\text{Be}({}^7\text{Li}, \alpha)$
15.7				${}^9\text{Be}({}^7\text{Li}, 2\alpha)$
17.7				${}^9\text{Be}({}^7\text{Li}, 2\alpha)$

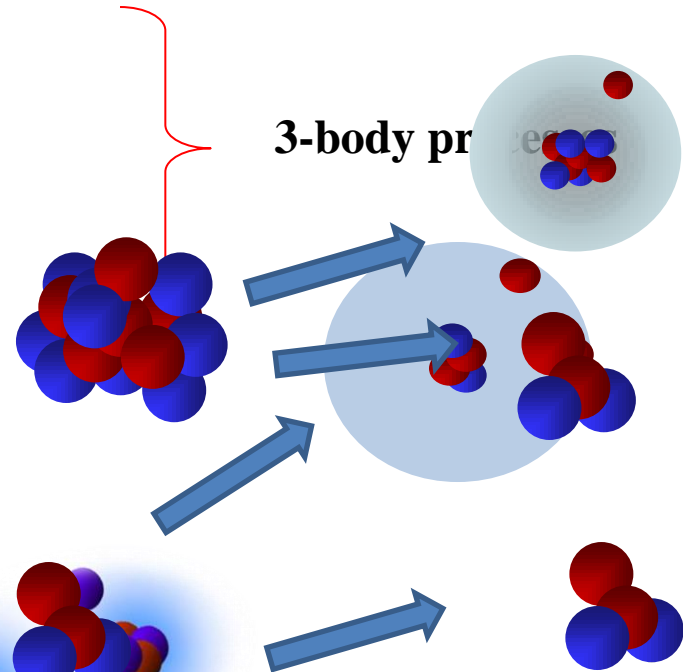
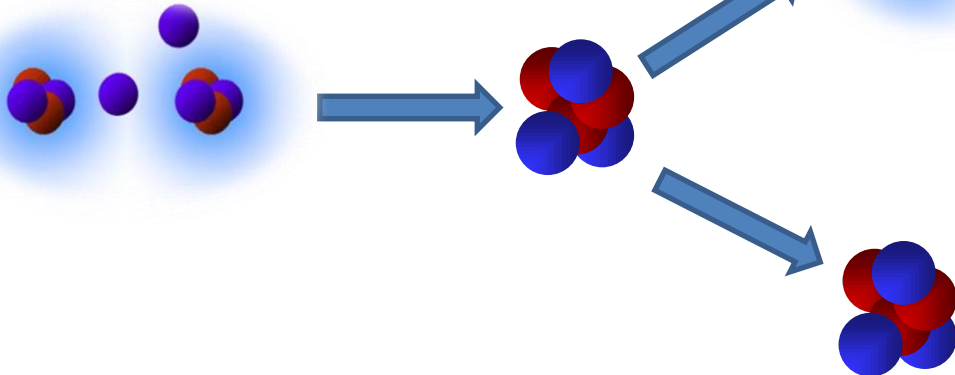
Resonant particle spectroscopy:

- transfer and decay into the constituents
- inelastic scattering followed by break up

Ex: $^{10}\text{Be} + ^9\text{Be} \rightarrow ^{15}\text{C}^* + \alpha$

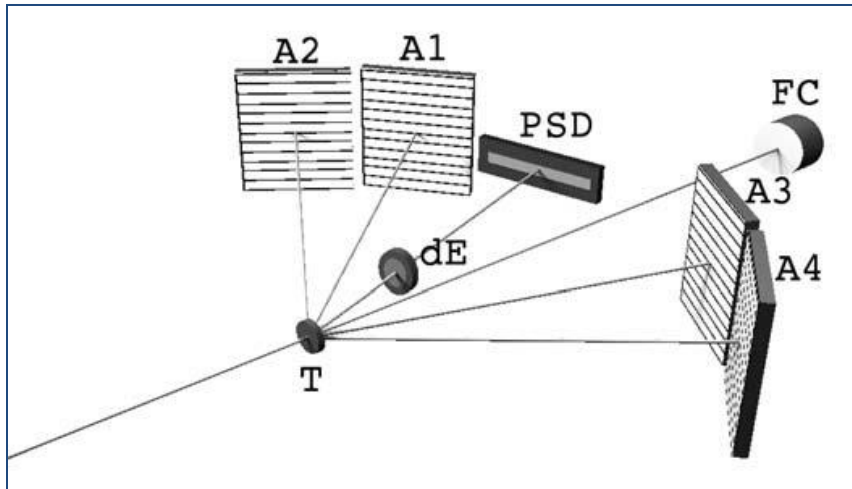
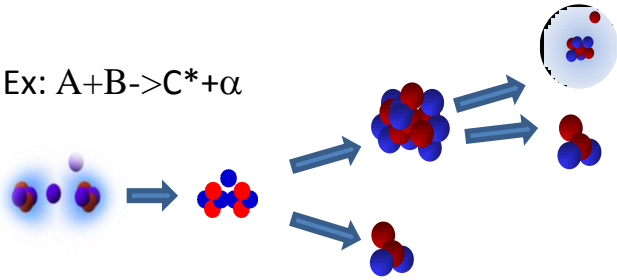


Ex: $^{10}\text{Be} + b \rightarrow ^6\text{He} + \alpha + b$

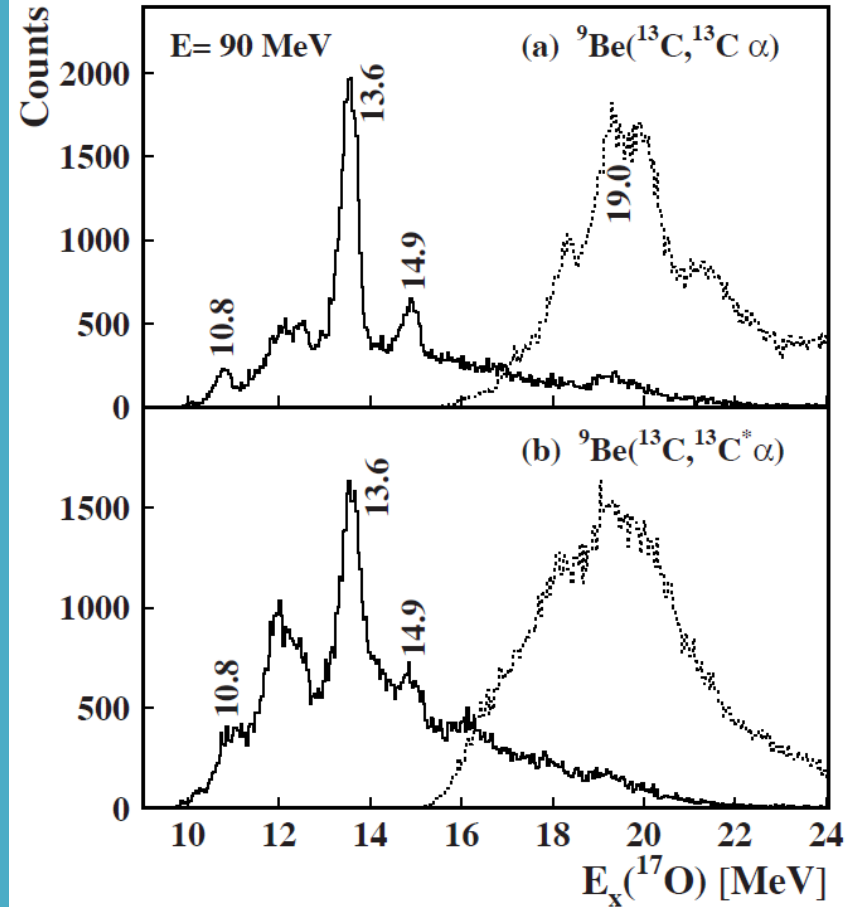


Resonant particle spectroscopy

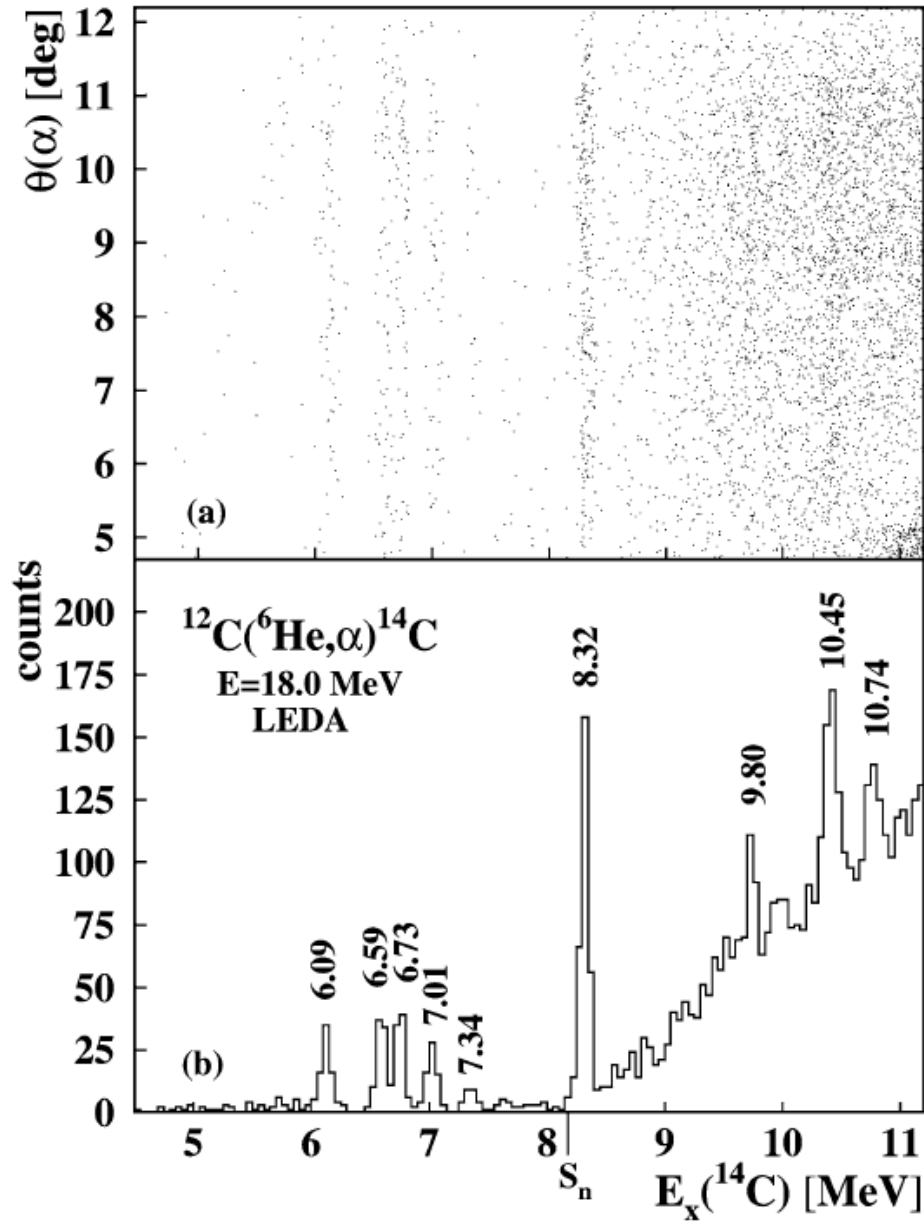
Ex: $A+B \rightarrow C^* + \alpha$



The detection of break-up products select states with large partial widths for decaying into a chosen channel thus enabling the selection of states with well-developed cluster structure. High segmentation of the detection system allows for high resolution measurement.



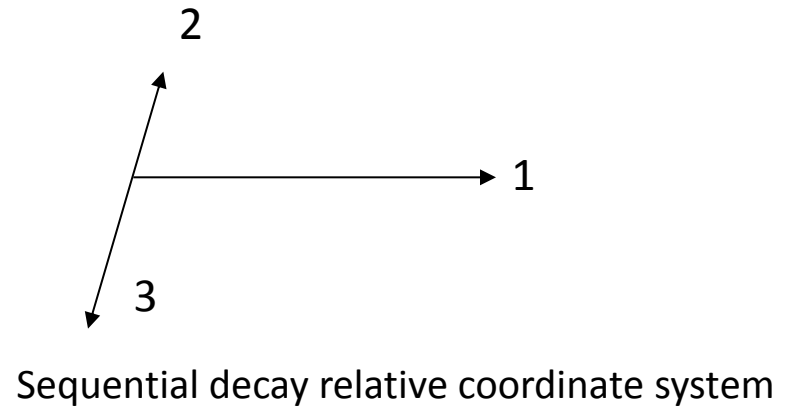
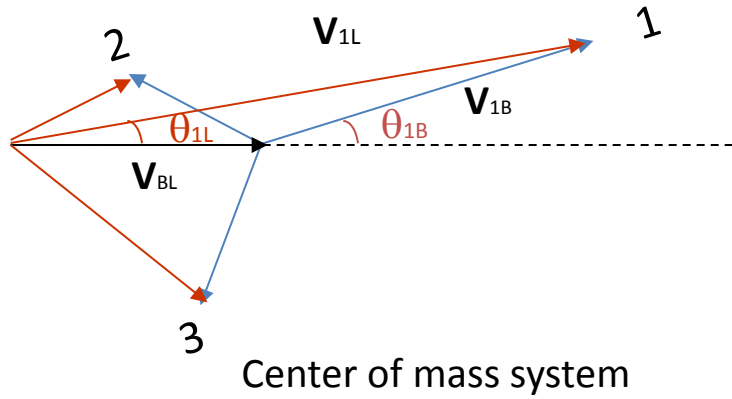
M. Milin et al. EPJ A41(2009)335



Three body kinematics

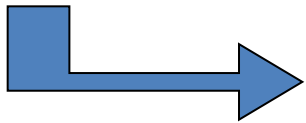
Three body kinematics

Reaction: $P+T \rightarrow 1+2+3$



$$V_{BL} = (2m_P E_{PL})^{1/2} / (m_P + m_T)$$

$$V_{1B}^2 = V_{1L}^2 + V_{BL}^2 - 2V_{1L}V_{BL}\cos\theta_{1L}$$



$$E_{1B} = \frac{1}{2}m_1 V_{1L}^2 + \underbrace{m_1(m_P E_{PL}) / (m_P + m_T)^2 - m_1 V_{1L} (2m_P E_{PL})^{1/2} / (m_P + m_T) \cos\theta_{1L}}_{a_1^2}$$

$$E_{1B} = E_{1L} - 2a_1 E_{1L} \cos\theta_{1L} + a_1^2$$

$$\cos \theta_{1B} = \frac{\sqrt{E_{1L}} \cos \theta_{1L} - a_1}{\left[E_{1L} - 2a_1 \sqrt{E_{1L}} \cos \theta_{1L} + a_1^2 \right]^{\frac{1}{2}}}$$

$$\phi_{1B} = \phi_{1L}$$

$$E_{1L} = E_{1B} + 2a_1 \sqrt{E_{1B}} \cos \theta_{1B} + a_1^2$$

$$\sin \theta_{BB} = \sqrt{\left(\frac{m_b E_{bL}}{m_A E_{AL}} \right)} \sin \theta_{bL}$$

$$\sin \theta_{bB} = \left(\frac{E_{bL} / E_T}{D} \right) \sin \theta_{bL}$$

$$\cos \theta_{1L} = \frac{\sqrt{E_{1B}} \cos \theta_{1B} + a_1}{\left[E_{1B} + 2a_1 \sqrt{E_{1B}} \cos \theta_{1B} + a_1^2 \right]^{\frac{1}{2}}}$$

$$\phi_{1B} = \phi_{1L}$$

If we detect particle one the kinematics is completely determined by the two body (particle 1 and 23) kinematics.

If we detect particle 2 and 3 we have to reconstruct the excitation energy of particle 23.

$$E_{Tot} = Q_{3body} + \underbrace{\frac{m_T}{m_P + m_T} E_P^L}_{E_{cm}} = E_{1-23} + E_{2-3}$$

Total energy available in the center of mass system

m_1 =mass of particle 1

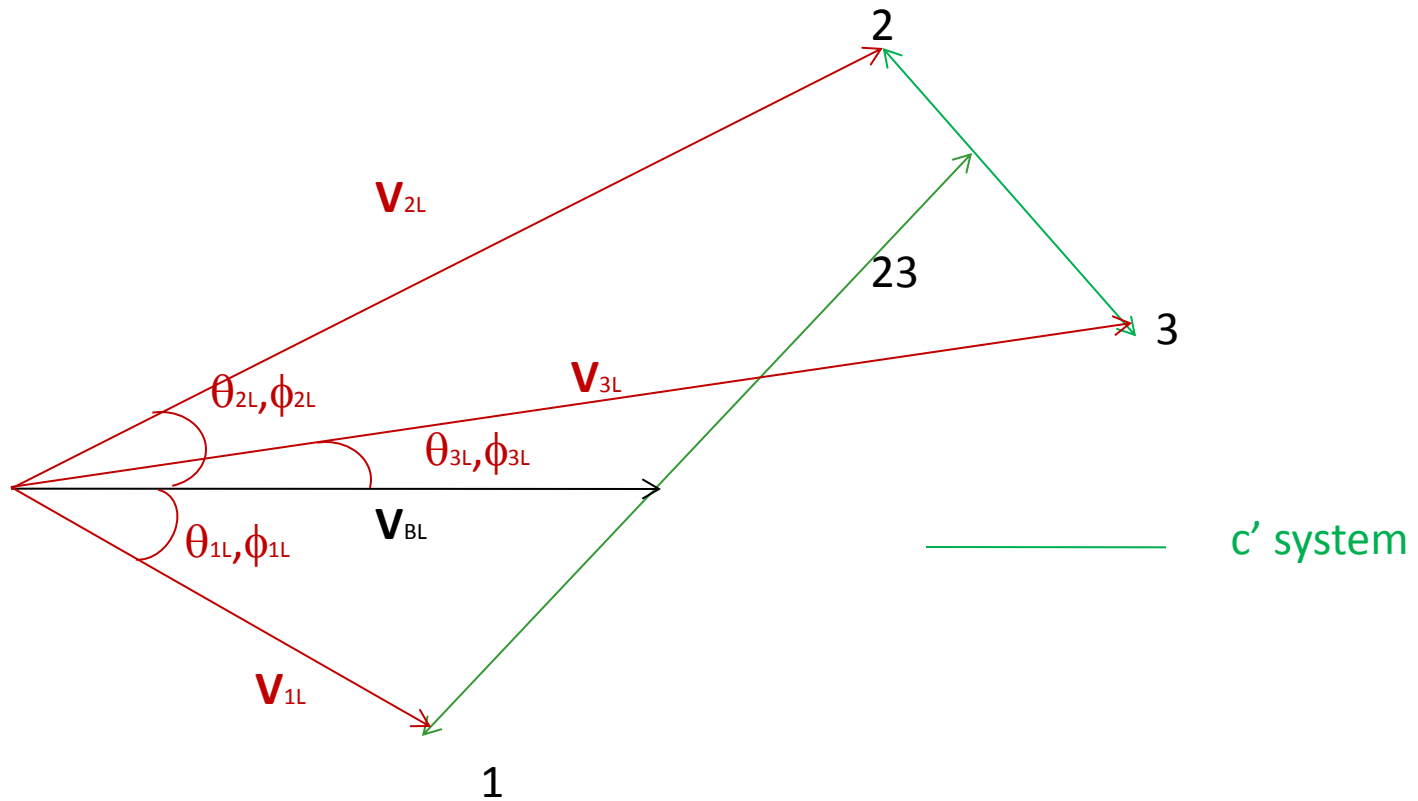
m_{23} = m_2+m_3 = mass of particle 23

M = $m_1+m_2+m_3$

We define the reduced masses:

μ_{1-23} = $m_1 m_{23} / (m_1 + m_{23}) = m_1 (m_2 + m_3) / M$

μ_{2-3} = $m_2 m_3 / (m_2 + m_3)$

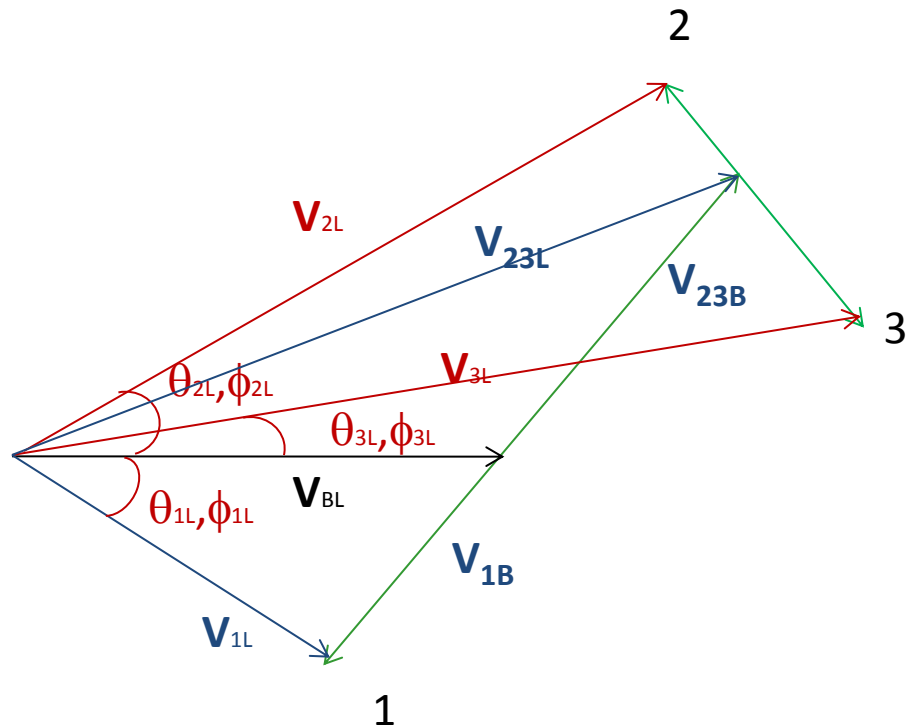


Measured quantities are $E_{1L}, \theta_{1L}, \phi_{1L} - E_{2L}, \theta_{2L}, \phi_{2L} - E_{3L}, \theta_{3L}, \phi_{3L}$ of one, two or even three particles

NB: we note that the velocity vectors are in the 3 dimensional space not in plane and both θ and ϕ angles are important.

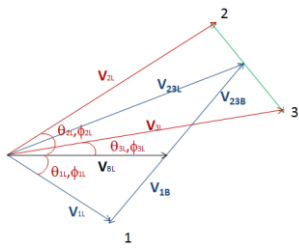
Eg. One wants to reconstruct excitation energy of particle 23

Reaction $p+T \rightarrow 1+23^* \rightarrow 1+2+3$
 e.g. : $\alpha+{}^6\text{Li} \rightarrow \alpha+{}^6\text{Li}^* \rightarrow \alpha+\alpha+d$



From two body kinematics one can reconstruct the excitation energy of the intermediate 23 system.
 See equations for two body kinematics

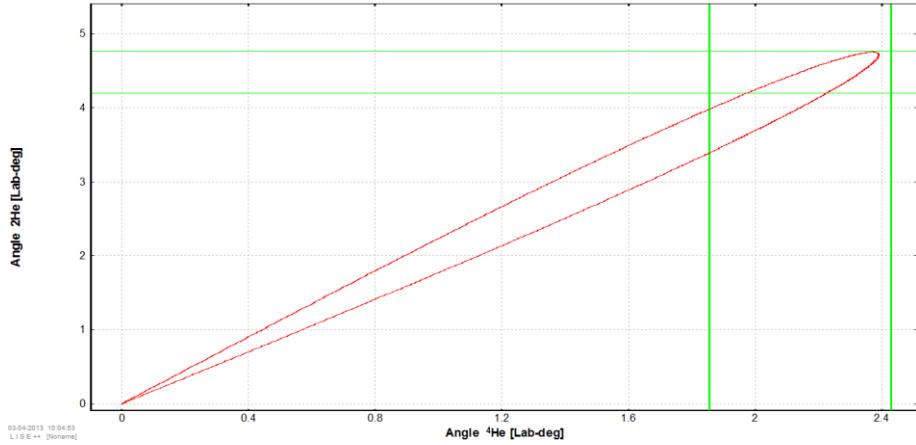
$$E_{\alpha B} + E_{6\text{Li}B} = E_{cm} - E_{6\text{Li}}^* + Q_{2\text{body}(\alpha-6\text{Li})}$$



$E^*({}^6\text{Li}) = 2 \text{ MeV}$

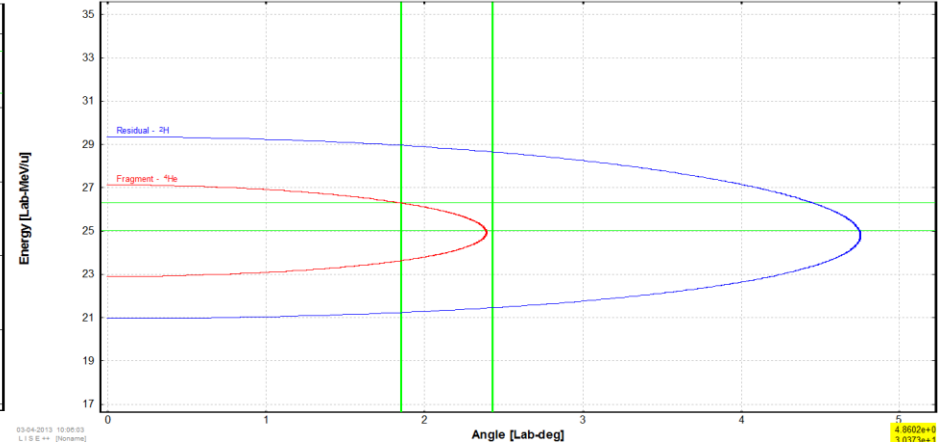
Reaction's Kinematics: A_lab & A_lab

${}^6\text{Li} \Rightarrow {}^4\text{He} + {}^2\text{H} \quad x({}^6\text{Li}, {}^4\text{He}+{}^2\text{H})x$; Reaction at the "middle" of the target
 Projectile Energy at the reaction place: 24.98 MeV/u
 Q reaction : 0.53 MeV (Excitations 2.0=>0.0+0.0); Plotted Energy option is "after reaction"



Reaction's Kinematics: A_lab & E_lab

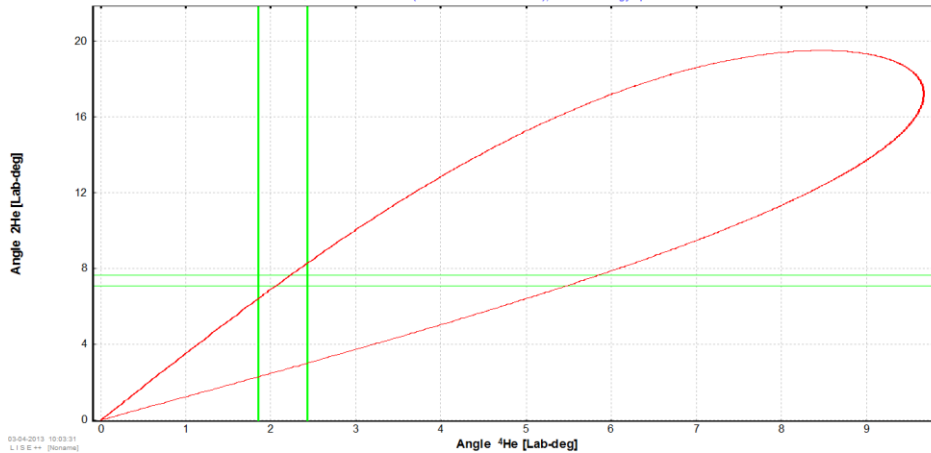
${}^6\text{Li} \Rightarrow {}^4\text{He} + {}^2\text{H} \quad x({}^6\text{Li}, {}^4\text{He}+{}^2\text{H})x$; Reaction at the "middle" of the target
 Projectile Energy at the reaction place: 24.98 MeV/u
 Q reaction : 0.53 MeV (Excitations 2.0=>0.0+0.0); Plotted Energy option is "after reaction"



$E^*({}^6\text{Li}) = 10 \text{ MeV}$

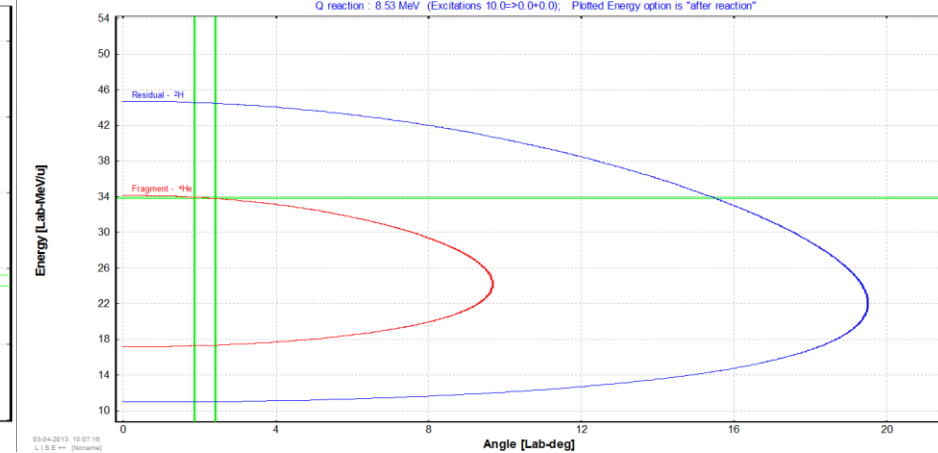
Reaction's Kinematics: A_lab & A_lab

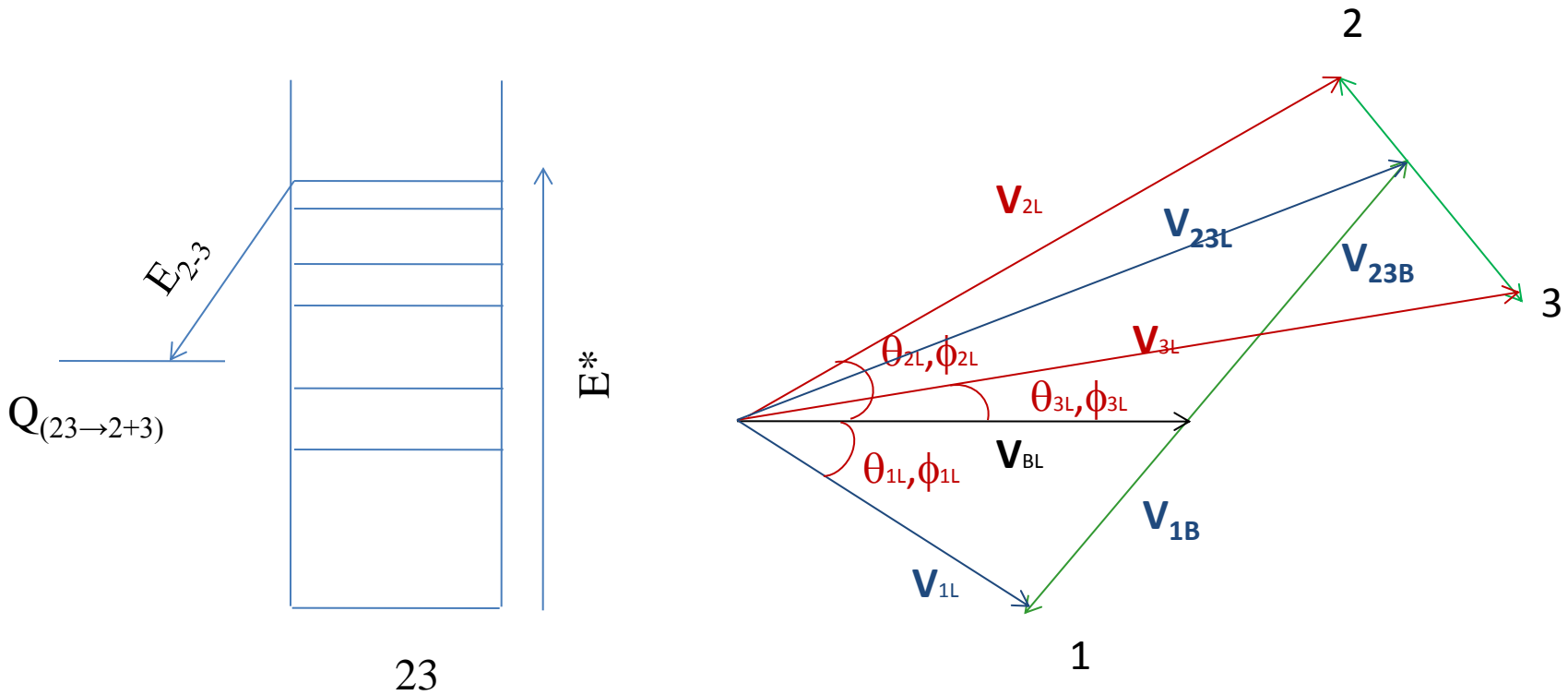
${}^6\text{Li} \Rightarrow {}^4\text{He} + {}^2\text{H} \quad x({}^6\text{Li}, {}^4\text{He}+{}^2\text{H})x$; Reaction at the "middle" of the target
 Projectile Energy at the reaction place: 24.98 MeV/u
 Q reaction : -8.53 MeV (Excitations 10.0=>0.0+0.0); Plotted Energy option is "after reaction"



Reaction's Kinematics: A_lab & E_lab

${}^6\text{Li} \Rightarrow {}^4\text{He} + {}^2\text{H} \quad x({}^6\text{Li}, {}^4\text{He}+{}^2\text{H})x$; Reaction at the "middle" of the target
 Projectile Energy at the reaction place: 24.98 MeV/u
 Q reaction : 8.53 MeV (Excitations 10.0=>0.0+0.0); Plotted Energy option is "after reaction"





$$E_{2-3} = E_{23}^* + Q_{(23 \rightarrow 2+3)} = 1/2 \mu v_{\text{rel}(2-3)}^2 = 1/2 \mu (\mathbf{V}_{2L} - \mathbf{V}_{3L})^2$$

quantities to be measured

quantity we want to extract from the experiment

$$\mathbf{V}_{2L} \rightarrow V_{2L}, \theta_{2L}, \phi_{2L} \quad \mathbf{V}_{3L} \rightarrow V_{3L}, \theta_{3L}, \phi_{3L}$$

$$\begin{cases} V_{2Lx} = V_{2L} \sin\theta_{2L} \cos\phi_{2L} \\ V_{2Ly} = V_{2L} \sin\theta_{2L} \sin\phi_{2L} \\ V_{2Lz} = V_{2L} \cos\theta_{2L} \end{cases}$$

$$V_{rel}^2 = (\mathbf{V}_{2L} - \mathbf{V}_{3L})^2 = V_{2L}^2 + V_{3L}^2 - 2 \mathbf{V}_{2L} \cdot \mathbf{V}_{3L}$$

$$V_{2L} = \sqrt{\frac{2E_{2L}}{m_2}} \quad V_{3L} = \sqrt{\frac{2E_{3L}}{m_3}}$$

$$\begin{cases} V_{3Lx} = V_{3L} \sin\theta_{3L} \cos\phi_{3L} \\ V_{3Ly} = V_{3L} \sin\theta_{3L} \sin\phi_{3L} \\ V_{3Lz} = V_{3L} \cos\theta_{3L} \end{cases}$$

$$\begin{aligned} \mathbf{V}_{2L} \cdot \mathbf{V}_{3L} &= \cancel{V_{2L}} \cancel{V_{3L}} \cos\theta_{rel} = \\ & V_{2Lx} V_{3Lx} + V_{2Ly} V_{3Ly} + V_{2Lz} V_{3Lz} = \\ & \cancel{V_{2L}} \sin\theta_{2L} \cos\phi_{2L} \cancel{V_{3L}} \sin\theta_{3L} \cos\phi_{3L} + \cancel{V_{2L}} \sin\theta_{2L} \sin\phi_{2L} \cancel{V_{3L}} \sin\theta_{3L} \sin\phi_{3L} + \cancel{V_{2L}} \cos\theta_{2L} \cancel{V_{3L}} \cos\theta_{3L} \end{aligned}$$

$$V_{rel}^2 = \frac{2E_{2L}}{m_2} + \frac{2E_{3L}}{m_3} - 2 \cos\theta_{rel}$$

$$E_{2-3}^* = \frac{1}{2} \mu_{2-3} V_{rel}^2 - Q_{23 \rightarrow 2-3}$$

measured quantities **energies** and **angles**

Summary and conclusions

Cluster structures can be measured in various way.

Resonant elastic scattering gives the possibility to measure the excitation function in a single run without changing beam energy. Particularly useful in RIB experiments.

With this technique only unbound states can be measured and the main limitation is the minimum resonance width that can be measured.

Both single particle and cluster states can be studied with RSM.

Resonant particle spectroscopy is the most commonly used technique to study cluster structure.

Good energy and angular resolution is required.